J Solid State Electrochem (1999) 3: 406–411

ORIGINAL PAPER

Ursula Rammelt · Sven Bischoff · Mohamed El-Dessouki
Renate Schulze · Waldfried Plieth · Lother Dunsch

Semiconducting properties of polypyrrole films in aqueous solution

Received: 28 July 1998 / Accepted: 22 February 1999

Abstract The influence of the nature of the anions on the conductivity of polypyrrole films in aqueous solution was investigated by photocurrent spectroscopy combined with electrochemical impedance spectroscopy in dependence on the potential. As demonstrated, the conductivity of polypyrrole films at negative potentials can vary from a semiconducting to an ionic conducting state, depending on the size of the charge-compensating counter-anion incorporated during the electropolymerization. The reduced polypyrrole shows semiconducting properties when small anions are inserted, releasing the polymer matrix during the reduction process. The polymer can than be considered as a two-layer system, consisting of a semiconducting layer and a porous layer. Measurements at different thickness of polypyrrole films have shown that the position of the semiconducting layer is in the electrode/polymer interface. The ohmic resistance of the semiconducting layer is in the range 1–5 kΩ, the capacitance approaches a value of 100–500 nF and the flatband potential is −0.62 V_{SCE}. If large anions are incorporated, cation insertion takes place during reduction, the electrolyte content in the polymer then is relatively high and the polymer's behaviour is similar to that of an ionic conductor. The results are presented and discussed together with the example of methylsulfonate as a relatively small anion and polystyrenesulfonate as a large anion.

Key words Polypyrrole · Anion influence · Film thickness · Photocurrent · Impedance spectroscopy

U. Rammelt · S. Bischoff · M. El-Dessouki
R. Schulze · W. Plieth (✉)
Dresden University of Technology,
Department of Chemistry,
Institute of Physical Chemistry and Electrochemistry,
Mommsenstrasse 13, D-01062 Dresden, Germany

L. Dunsch
Institut für Festkörper-
und Werkstofforschung
Helmholtzstrasse 20, D-01171 Dresden, Germany

Introduction

Conducting polymer-modified electrodes have been the subject of a great deal of recent investigation [1–3]. Among these polymers, polypyrrole (PPy) is of particular interest since films can be formed from aqueous solutions, resulting from the relatively low oxidation potential of the pyrrole monomers [4]. It is well known that the electrochemical properties of PPy are essentially dependent on the nature of the solvent, the composition of the electrolyte and the conditions of synthesis of PPy [5–9]. Electrochemically prepared PPy was shown to have an oxidized (doped) matrix, which incorporates the anion of the supporting electrolyte for charge compensation. The electrochemical switching of PPy between the doped (conducting) and undoped (neutral) states involves both electron and ion transport within the film. Most of the recent investigations into the mechanism of PPy-film coated electrodes have centred around this reduction/oxidation of the polymer, especially with respect to the mass/charge transport process within the porous film [10–13]. The transport process and the conductivity of PPy-film coated electrodes have been measured as a function of oxidation level, where in most cases the properties have been investigated in a potential range from the fully oxidized state to the slightly reduced one. If the polymer is reduced at very negative potentials, the PPy is expected to behave like a semiconductor. Although semiconducting properties can be well studied by photocurrent measurements, there are relatively few studies on the photoelectrochemical behaviour of conducting polymers [14–16].

In this paper we want to focus on the use of photocurrent spectroscopy combined with electrochemical impedance spectroscopy in order to determine the behaviour of the polymer during the electrochemical switching process, when the PPy-film coated electrode is in contact with an aqueous solution. The electrochemically deposited PPy will be doped with methylsulfonate as a relatively small anion and polystyrenesulfonate as a large anion.

Experimental

A one-compartment, three-electrode cell was employed for the synthesis and electrochemical analysis of the PPy films. An Au disc electrode (A = 0.785 cm^2) sealed in epoxy resin served as a working electrode and a Pt plate as counter electrode. All potentials are quoted with respect to the saturated calomel electrode (SCE) as being the reference electrode. PPy films were synthesized potentiodynamically (E = 0.70–0.75 V_{SCE} at a constant sweep rate of dE/dt = 10 mV s^{-1}) from N_2 saturated aqueous solutions of 0.05 M pyrrole and 0.1 M electrolyte (either methylsulfonic acid, perchlorate acid or sodium polystyrenesulfonate) onto the Au electrode. This method has been optimized to obtain homogeneous and good quality films [17]. In general, the thickness of PPy films was 2 μm and was estimated by measuring the charge passed with the assumption that 24 mC cm^{-2} charge yielded 0.1 μm film [18].

The photocurrent was detected with a model 5208 lock-in amplifier coupled to a 197 light chopper (PAR, USA) and corresponding electrochemical instruments. The potentiostat used was a D6734 (HEKA electronic) and the light source came from a xenon lamp in conjunction with a grating monochromator.

The PPy was checked by cyclic voltammetry at 10 mV s^{-1} using a PAR model 273 potentiostat-galvanostat before and after photocurrent and impedance measurements. The PPy-film coated electrodes were cycled until a constant voltammogram was reached. Impedance measurements were carried out in a monomer-free solution with the IM5d impedance measurement system of Zahner-electric. An ac amplitude of 5 mV was applied and data were collected in the frequency range 100 kHz–0.1 Hz using 10 points per decade. For each film, impedance spectra were obtained at potentials between 0.4 V_{SCE} and −1.0 V_{SCE} in steps of 50–200 mV. Films were allowed to equilibrate for 12 min at each potential before being measured.

All measurements were carried out in a shielded dark box at room temperature.

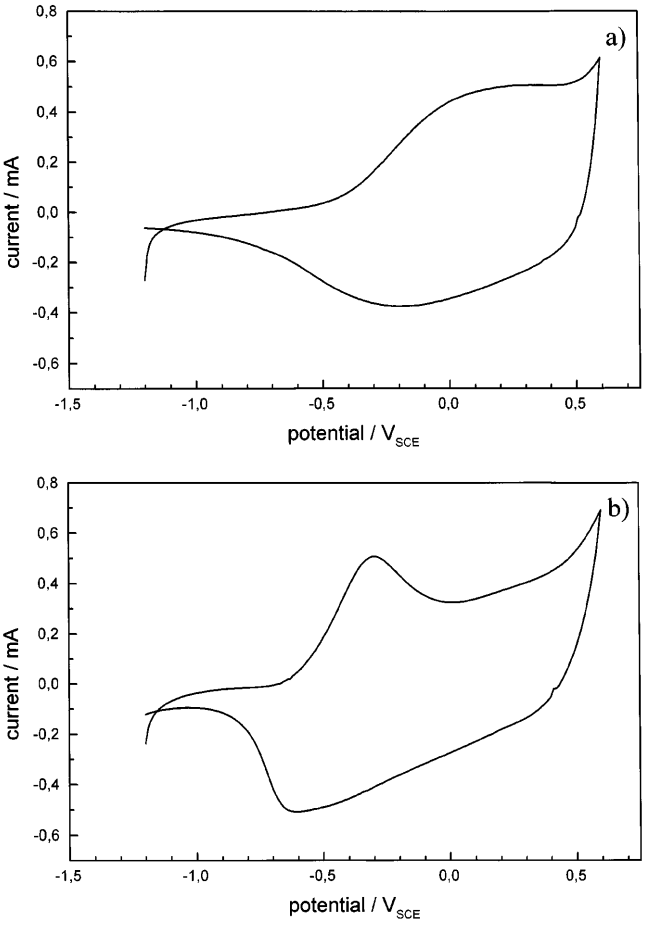

Fig. 1 Cyclic voltammogram for **a** PPy(MS) electrode in 0.1 M NaMS solution **b** PPy(PSS) electrode in 0.1 M NaPSS solution; stationary curve (3rd scan); scan rate 10 mVs^{-1}

Results and discussion

Cyclic voltammetry

The electrochemical behaviour of PPy doped with methylsulfonate [PPy(MS)] and PPy doped with polystyrenesulfonate [PPy(PSS)] was investigated in 0.1 M solutions of sodium methylsulfonate (NaMS) and sodium polystyrenesulfonate (NaPSS), respectively. Typical cyclic voltammograms for both PPy films are shown in Fig. 1.

The different shapes of the two voltammograms indicate different situations with respect to the counterion exchange in these films. As described in the literature [19–22], PPy films prepared with small or medium-sized anions such as MS^- exhibit a predominant anion exchange, whereas PPy films prepared with large polymeric anions such as PSS^- produce a predominant cation exchange during the oxidation-reduction process. For comparison, PPy was also prepared in 0.1 M $HClO_4$ and reduced in 0.1 M tetra-*n*-butylammonium bromide (TBABr) solution. In this case the incorporation of cations at negative potentials is prevented.

Information on the relative contribution of anion and cation exchange processes and their influence on the conductivity of PPy films can be obtained by photocurrent and impedance measurements.

Photocurrent measurements

Figure 2 shows the photocurrent-potential characteristics of PPy films prepared with different anions. In the case of PPy(MS), the onset potential for a cathodic photocurrent is about −0.5 V_{SCE}, which corresponds to the cathodic peak potential in the voltammogram of Fig. 1. With progressing reduction the photocurrent rises, then at more negative potentials it decreases again. MS^- is a medium-sized anion where only the ions shallowly trapped near the surface of the polymer chain can release the PPy during the reduction process. Other ions are deeply trapped in the chains and therefore the further reduction process is accompanied by cation insertion [6, 19, 20, 23]. The increasing insertion of cations should be the reason for the decreasing photocurrent.

The behaviour should be explained with the assumption that the reduced PPy can be considered as a two-layer system, consisting of a more compact layer and a porous layer, where the position of the semiconducting layer is in the more compact layer at the electrode/polymer interface [16, 24] rather than in the polymer/electrolyte interface [25]. This means the pho-

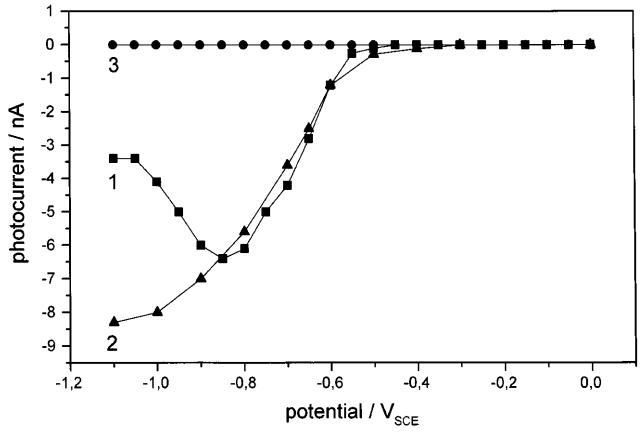

Fig. 2 Photocurrent-potential response for PPy films prepared with *1* MS, measured in 0.1 M NaMS solution, *2* ClO_4^-, measured in 0.1 M tetra-*n*-butylammonium bromide solution, *3* PSS, measured in 0.1 M NaPSS solution

tons have to pass through the porous polymer bulk to reach the space charge region where the photogenerated charge pairs are separated by the electric field. Part of the photons are absorbed out of this region and do not contribute to the photocurrent, because with the progressing reduction process the increasing number of cations within the porous layer provide recombination centres for the photogenerated charge pairs. If this assumption is true, the photocurrent should not decrease if the insertion of cations into the PPy films is hindered. Therefore PPy films were prepared with a small anion (ClO_4^-). After the electropolymerization, the photocurrent measurements were carried out in TBABr solution with a bulky cation in order to avoid the insertion of cations during discharging. On negative-going scans the electroneutrality is only preserved through a release of anions and therefore the photocurrent does not decrease (see Fig. 2, curve 2).

The two-layer model is also in agreement with the behaviour of PPy(PSS). The polymeric PSS^- anions are bound to the polymer matrix and during the reduction process Na^+ ions must move into the film for charge compensation. Consequently, at more negative potentials the electrolyte content in the polymer is increased. The layer can be considered as an ionic conductor, the formation of a semiconducting layer is not possible and therefore a photocurrent cannot be observed over the whole potential range (Fig. 2, curve 3).

Further insight into the role of counterions during the reduction process should be given by impedance measurements.

Impedance measurements

Polypyrrole + methylsulfonate

Figure 3 shows typical impedance plots for a PPy(MS) film in 0.1 M NaMS solution at various potentials

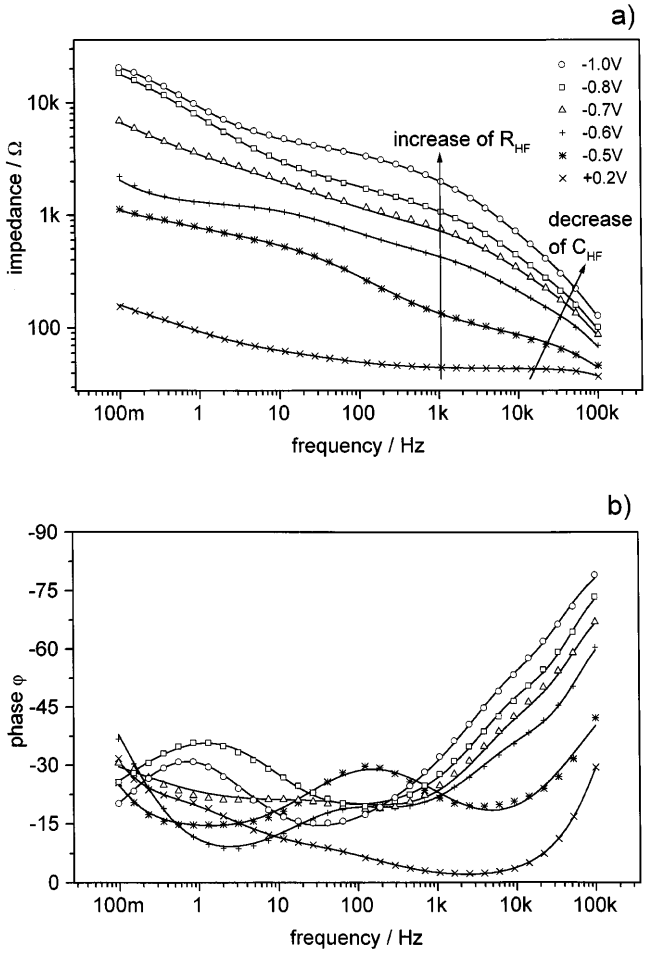

Fig. 3 Bode plots for a PPy(MS) film at different potentials: **a** modulus of impedance, **b** phase shift (solid lines are the fit to the measured points)

during the reduction of the polymer. The impedance spectra were obtained in the potential range of 0.4 to −1.0 V_{SCE}. From 0.4 to −0.2 V_{SCE} the impedance behaviour can be analyzed using a modified transmission line model introduced by Albery et al. [26, 27], in which the electronic and ionic conduction through the conducting polymer is described (see the right part of Fig. 4a) by a model including two resistances R_e and R_i and a distributed capacitance C_F which connects the two resistive lines; R_e and R_i describe the movement of the electrons in the polymer chains and of ions in the aqueous pores, respectively; C_F arises from the oxidation and reduction of the polymer backbone. As the potential is decreased below −0.2 V_{SCE} a more complex model is required because at high frequencies a new semicircle (time constant *RC*) is observed, marked by the arrows in Fig. 3. The introduction of this high-frequency semicircle into the impedance plot was also seen by Albery and Mount [28], Pickup and co-workers [29, 30] and Deslouis et al. [31] and leads to the complex transmission line model given in Fig. 4.

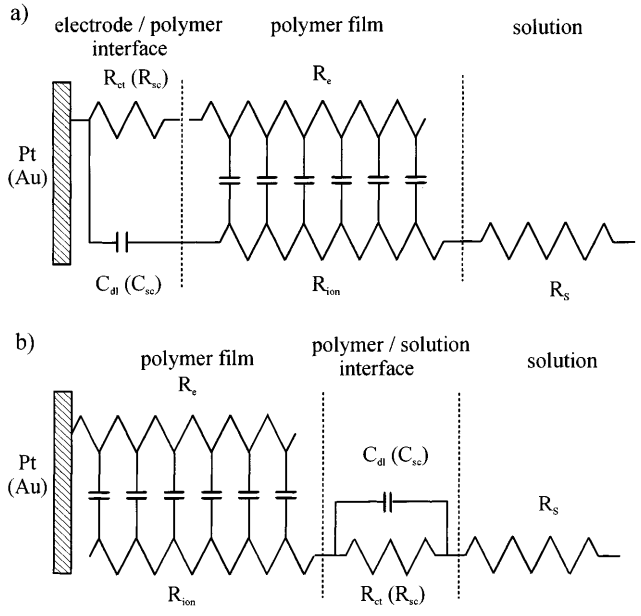

Fig. 4 Equivalent circuit with charge transfer resistance R_{ct} and double-layer capacitance C_{dl} at the **a** electrode/polymer and **b** polymer/solution interface according to [30]

According to the authors, the high-frequency time constant may be attributed to a charge-transfer resistance in parallel with a double-layer capacitance at either the electrode/polymer or the polymer/electrolyte interface. Ren and Pickup [30] state that the high-frequency time constant originates from a process at the electrode/polymer interface. Their argument is that the value of C_{dl} is approximately the same as the value of the Pt double-layer capacitance ($\cong$23 μF cm^{-2}) and R_{ct} increases with decreasing potential. This is expected for an electron transfer resistance at an electrode surface but not for an ion transfer resistance at the polymer/electrolyte interface.

In this paper we want to focus on the investigation of this high-frequency behaviour of PPy-film coated electrodes in order to explain why a photocurrent can be observed in the case of PPy(MS) but not in the case of PPy(PSS).

It should be mentioned that all capacitances used in the equivalent circuit are not ideal and the deviation from the ideal behaviour is taken into consideration using a constant phase element (CPE) [32]:

$$Z_{CPE} = A_{CPE}(j\omega)^{-n}$$

The appearance of the CPE element is often related to the electrode roughness or, in the case of dielectric layers like coatings, passive layers, etc., to the inhomogenity in the conductance or dielectric constant inside the layer [33, 34]. The exponent n of the CPE element can be regarded as a measure of the inhomogenity of the PPy film.

Figure 5 shows the high-frequency resistance R_{HF} and high-frequency capacitance C_{HF} of a PPy(MS) film

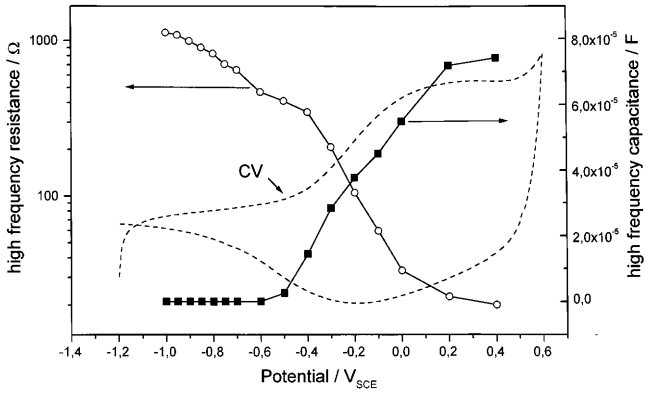

Fig. 5 Change of high-frequency resistance R_{HF} (○) and high-frequency capacitance C_{HF} (■) of PPy(MS) with the potential. The cyclic voltammogram (CV) is shown for comparison

in dependence on the potential. A larger value of the high-frequency time constant is observed at potentials more negative than −0.2 V_{SCE} where the cathodic current peak appears in the cyclic voltammogram. The values of R_{HF} increase with decreasing potentials, as expected according to the assumption of Ren and Pickup [30]. In the same way, the values of C_{HF} sharply decrease from about 35 μF cm^{-2} at −0.2 V_{SCE} to about 30 nF cm^{-2} at −1.0 V_{SCE}. These small values of C_{HF} correspond rather to a semiconductor capacitance than a metal double-layer capacitance. In order to test this high-frequency capacitance, the inverse of the square of C_{HF} is plotted against the potential in a Mott-Schottky diagram (Fig. 6). In the region of −0.6 V to −0.85 V_{SCE} a linear relationship between $1/C^2$ and the potential E was observed, meaning that the polymer has semiconductor properties and the high-frequency capacitance C_{HF} is similar to a space-charge capacitance C_{CS} which obeys the Mott-Schottky equation:

$$\frac{1}{C_{sc}^2} = \frac{2}{\varepsilon\varepsilon_0 N_0 e}\left(E - E_{FB} - \frac{kT}{e}\right)$$

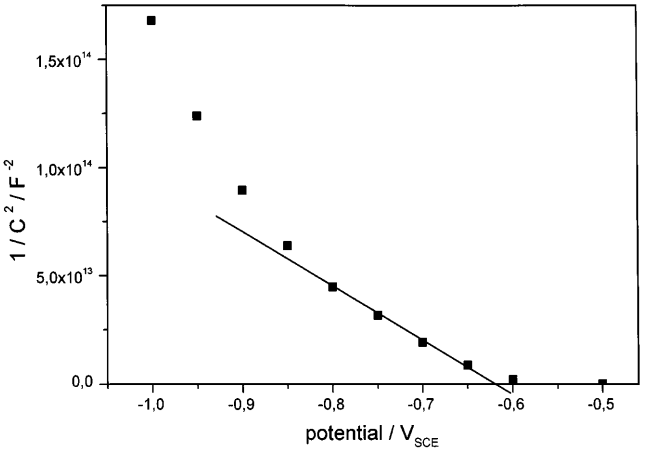

Fig. 6 Mott-Schottky plot of PPy(MS) in the reduced state

where ε is the dielectric constant of the polymer, ε_0 the permittivity of free space, N_0 the charge carrier density and E_{FB} the flatband potential. The interception of the straight line with the x axis provides a flatband potential of $E_{FB} = -0.62\ V_{SCE}$, and the slope of the straight line obtained yields $N_0 = 2 \times 10^{16}\ cm^{-3}$ (with the assumption that $\varepsilon = 10$). The flatband potential corresponds to the onset potential of the photocurrent in Fig. 2. In the same way as the photocurrent decreases at potentials more negative than $-0.85\ V_{SCE}$, the linear relationship between $1/C^2$ and E becomes lost.

The exponent n of the CPE element varies from about 0.7 in the oxidized state of the polymer to 0.85 in the reduced state, with a sharp decrease ($n = 0.63$) near the flatband potential. This behaviour could be explained with the build-up of the space-charge region at the electrode/polymer interface at E_{FB}. Therefore, the high-frequency time constant changes from a double-layer capacitance in parallel with a charge-transfer resistance to a space-charge capacitance in parallel with a space-charge resistance (see Fig. 4a).

Polypyrrole + polystyrenesulfonate

A series of impedance measurements was also made for PPy(PSS)-film coated electrodes in 0.1 M NaPSS solution in the potential range of 0.4 V to $-1.0\ V_{SCE}$ (Fig. 7). At negative potentials a second time constant develops in the high-frequency range of the Bode plot. The same behaviour was observed by Ren and Pickup [30] with PPy(PSS)-film coated electrodes in aqueous $NaClO_4$ solution.

Using the same equivalent circuit as for PPy(MS), different behaviour for PPy(PSS) and PPy(MS) was observed (compare Fig. 3 with Fig. 7). At potentials more negative than $-0.3\ V_{SCE}$ the electronic conductivity decreases owing to the reduction of the polymer. However, in contrast to the PPy(MS)-film coated electrode, the decrease of electronic conductivity is associated with an increase of ionic conductivity because of the moving of Na^+ into the film during the reduction process. At potentials more negative than $-0.8\ V_{SCE}$ the ionic conductivity is predominant and is reflected by a decrease of R_{HF} and an increase of the corresponding values of C_{HF} (Fig. 8).

The values of C_{HF} are in the range of 20–30 $\mu F\ cm^{-2}$, close to the bare electrode value of Au. This means that the C_{HF} is a double-layer capacitance and cannot be attributed to a space-charge capacitance. The values of the exponent n are in the range 0.86–0.90 in the whole potential range. In the case of PPy(PSS)-film coated electrodes, a parallel combination of double layer capacitance C_{dl} and charge-transfer resistance R_{ct} generates the high-frequency time constant and the behaviour can be well described by the equivalent circuit shown in Fig. 4a. Consequently, with PPy(PSS)-film coated electrodes, photocurrents cannot be observed over the whole potential range (see Fig. 2, curve 3).

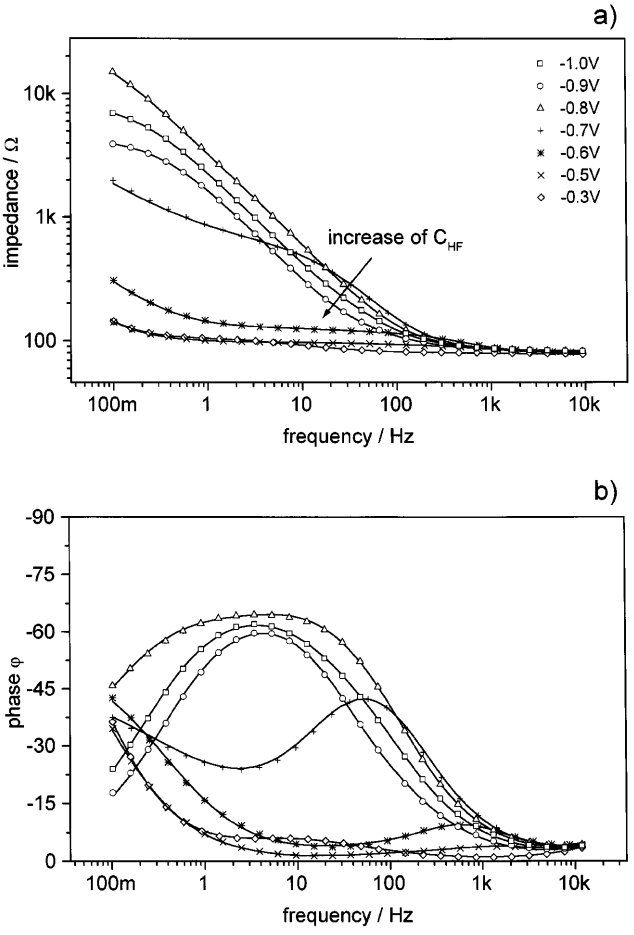

Fig. 7 Bode plots for a PPy(PSS) film at different potentials: **a** modulus of impedance, **b** phase shift (solid lines are the fit to the measured points)

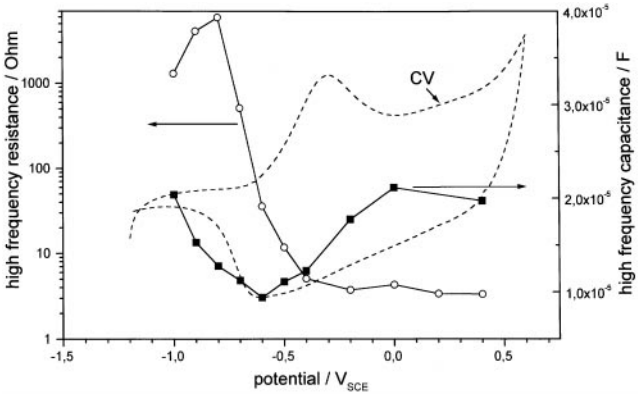

Fig. 8 Change of high-frequency resistance R_{HF} (○) and high-frequency capacitance C_{HF} (■) of PPy(PSS) with the potential (the CV is shown for comparison)

Influence of the film thickness on the semiconducting properties

With the assumption that the semiconducting layer is only a small part of the polymer film, the properties

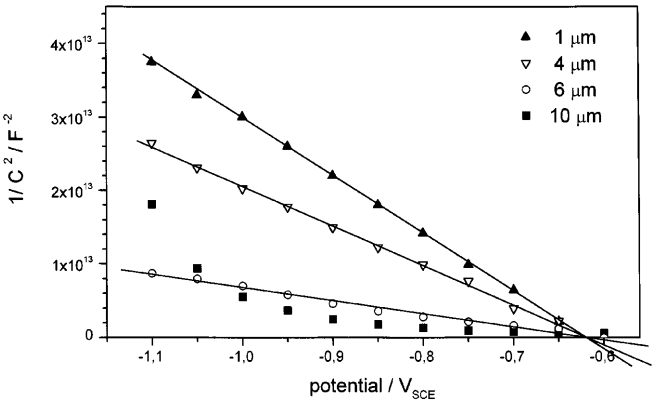

Fig. 9 Mott-Schottky plots at different thickness of $PPy(ClO_4)$ films

were influenced to a great extent by the porous layer. The experiments were made with PPy films containing ClO_4^- as counterions [$PPy(ClO_4)$] and the film thickness was varied from 1 μm to 10 μm by controlling the number of coulombs passed. The reduction was carried out in a N_2 saturated solution of 0.1 M TBABr in a potential range from −0.5 V to −1.0 V_{SCE}. After a waiting time of 12 min at each potential, the impedance measurement was started. Figure 9 shows the dependence of C_{sc} on the film thickness. With increasing thickness the Mott-Schottky slope is lowered. This behaviour can be correlated with an increase of the charge carrier density N_0. However, if the film thickness is approximately 10 μm, the waiting time of 12 min is too short to reach the redox equilibrium. Therefore an increasing number of deeply trapped anions remains in the polymer and affects the movement of the positive charges of the polymer backbone, thereby reducing the charge carrier density. The more negative the potential, the greater the number of remaining anions and the Mott-Schottky curve bends up.

Conclusion

The semiconducting properties of PPy-film coated electrodes in aqueous solution depend on the size of the counter-anion incorporated during the electropolymerization. In the reduced state the polymer consists of two layers, a compact (semiconducting) layer and a porous layer. The semiconducting layer can only be formed if the counter-anion is small and can release the polymer matrix during the reduction process. This behaviour can be deduced from the results of photocurrent and impedance measurements. The photocurrent-potential characteristics correspond to p-type semiconducting behaviour. From the measurements of the capacitance at high frequencies there results a flatband potential of $E = -0.62\ V_{SCE}$ and a charge carrier density of $N_0 = 2 \times 10^{16}\ cm^{-3}$.

References

1. Diaz AF, Bargon J (1986) In: Skotheim TA (ed) Handbook of conducting polymers. Dekker, New York, p 81
2. Heinze J (1990) In: Steckhan E (ed) Topics in current chemistry, vol 125. Springer, Berlin Heidelberg New York, p 2
3. Garnier F (1998) Chem Phys 227: 253
4. Asavapiriyanont S, Chandler GK, Gunawardena GA, Pletcher D (1984) J Electroanal Chem 177: 229
5. Ren X, Pickup PG (1993) J Phys Chem 97: 5356
6. Vorotyntsev MA, Vieil E, Heinze J (1996) Electrochim Acta 41: 1913
7. Zhong C, Doblhofer K (1990) Electrochim Acta 35: 1971
8. Otero TF, Sansinena JM (1996) J Electroanal Chem 412: 109
9. Garnier F, Yasser A, Hajlaoui R (1993) J Am Chem Soc 115: 8716
10. Buck RP (1986) J Electroanal Chem 210: 1
11. Vorotyntsev MA, Daikhin LI, Levi MD (1994) J Electroanal Chem 364: 37
12. Paulse CD, Pickup PG (1988) J Phys Chem 92: 7002
13. Jüttner K, Ehrenbeck C (1998) J Solid State Electrochem 2: 60
14. Kalaji M, Nyholm L, Peter LM, Rudge A-J (1991) J Electroanal Chem 310: 113
15. Peramunage D, Tomkiewicz M (1987) J Electrochem Soc 134: 1384
16. Abrantes LM, Correia JP (1996) Electrochim Acta 41: 1747
17. Ehrenbeck C, Jüttner K (1996) Electrochim Acta 41: 511
18. Diaz AF, Castillo JI, Logan JA, Lee WY (1981) J Electroanal Chem 129: 115
19. Silk T, Tamm J (1996) Electrochim Acta 41: 1883
20. Tanguyg J, Mermilliod M (1987) Synth Metals 20: 129
21. de Paoli M, Peres RCD, Panero S, Scrosati B (1992) Electrochim Acta 37: 1173
22. Bobacka J, Gao Z, Ivaska A (1994) J Electroanal Chem 368: 33
23. Ren X, Pickup PG (1995) J Electroanal Chem 396: 359
24. Semenikhin OA, Kazarinov VE (1994) Elektrokhimiya 30: 739
25. Miller DL, Bockris JO'M (1992) J Electrochem Soc 139: 967
26. Albery WJ, Chen Z, Horrocks BR, Mount AR, Wilson PJ (1989) Faraday Discuss Chem Soc 88: 247
27. Albery WJ, Elliot CM, Mount AR (1990) J Electroanal Chem 288: 15
28. Albery WJ, Mount AR (1994) J Chem Soc Faraday Trans 90: 1115
29. Duffitt GL, Pickup PG (1992) J Chem Faraday Trans 88: 1417
30. Ren X, Pickup PG (1997) J Electroanal Chem 420: 251
31. Deslouis C, Musiani MM, Tribollet B, Vorotyntsev MA (1995) J Electrochem Soc 142: 1902
32. Rammelt U, Reinhard G (1990) Electrochim Acta 35: 1045
33. Göhr H (1981) Ber Bunsenges Phys Chem 85: 274
34. Rammelt U, Reinhard G (1995) Farbe Lack 101: 369